Audio Engineering Society

Convention Paper 9943

Presented at the 144th Convention
2018 May 23 – 26, Milan, Italy

Ambisonic decoding with panning-invariant loudness on small layouts (AllRAD2)

Franz Zotter and Matthias Frank

University of Music and Performing Arts, Graz – Institute of Electronic Music and Acoustics

Correspondence should be addressed to Franz Zotter (zotter@iem.at)

ABSTRACT

On ITU BS.2051 surround with height loudspeaker layouts, Ambisonic panning is practice-proof, when using AllRAD decoders involving imaginary loudspeaker insertion and downmix. And yet on the 4+5+0 layout, this still yields a loudness difference of nearly 3 dB when comparing sounds panned to the front with such panned to the back. AllRAD linearly superimposes a series of two panning functions, optimally sampled Ambisonics and VBAP. Both are perfectly energy-preserving and therefore do not cause the loudness differences themselves, but their linear superposition does. In this contribution we present and analyze a new AllRAD2 approach that achieves decoding of constant loudness by (i) superimposing the squares of both panning functions, and (ii) calculating the equivalent linear decoder of the square root thereof.

1 Introduction

Ambisonic decoding has been posing a topic of research for years, and for higher-order Ambisonic decoding, one can, e.g. find works by Daniel (max-r_E [1], on pseudo-inverse decoding [2]), by Poletti (robust panning laws and mode matching [3, 4, 5]), Zotter, Pomberger, Noisternig (energy-preserving decoding [6]), Batke, Keiler [7, 8], Zotter, Frank (AllRAD [9, 10, 11]), and about non-linear optimization designs of Moore, Wakefield [12], Scaini, Arteaga (IDHOA [13]), Heller, Benjamin [14, 15], Epain, Jin, Zotter (constant spread decoding [16]), but also notable works by Gerzon [17], Craven [18], and Wiggins [19].

On the 4+5+0 3D layout [20], All-Round Ambisonic Decoding (AllRAD [10]) permits to use the order $N = 5$ to support its dense frontal loudspeaker spacing.

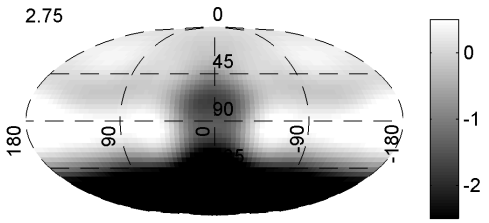

Fig. 1: Loudness E (dB) for 5th-order AllRAD, 4+5+0.

This paper discusses AllRAD because of its practical simplicity and its option to insert and downmix imaginary loudspeakers [21, 22, 23] to stabilize loudness. And yet, its use with 5th-order Ambisonics still yields a loudness difference of nearly $+3$ dB, when comparing loudnesses for panning to the back and to the front, see Fig. 1. This paper aims to amend this slight defect.

Alternatively, hemispherical energy-preserving Ambisonic decoding [6] focuses on a perfectly constant E measure for loudness. With $\mathrm{L}=9$ loudspeakers of the 4+5+0 layout, its constraint $\mathrm{L} \geq \frac{(\mathrm{N}+1)(\mathrm{N}+2)}{2}$ would however only permit orders up to $\mathrm{N} \leq 2$, an impractically poor resolution on the frontal loudspeakers.

Before addressing decoding, we begin discussing *panning functions*, Gerzon's E and $\boldsymbol{r}_\mathrm{E}$ measures [17] for loudness and localization. The *virtual Ambisonic panning function* achieves ideal measures that AllRAP/AllRAD tries to turn into an *Ambisonic panning function* by integrating over a vector-base amplitude panning (VBAP [24]) *discretization kernel* with imaginary loudspeakers and downmix.

The new AllRAD2 approach tested and presented here aims at keeping the practical advantages of AllRAD while perfecting a panning-invariant loudness on irregular loudspeaker layouts containing strongly varying distances between neighboring loudspeakers. For the 4+5+0 layout AllRAD2 reduces the loudness difference indicated by the E measure from 2.75 dB to 0.22 dB.

2 Amplitude panning

Amplitude panning employs a *panning function* g_l expressing an amplitude factor yielding the *surround signal* x_l from a mono input $s(t)$ for each of the $l=1\ldots\mathrm{L}$ loudspeakers

$$x_l(t) = g_l(\boldsymbol{\theta}_\mathrm{s})\, s(t). \tag{1}$$

The panning function is controlled by the panning direction $\boldsymbol{\theta}_\mathrm{s} = [\cos\varphi_\mathrm{s}\sin\vartheta_\mathrm{s}, \sin\varphi_\mathrm{s}\sin\vartheta_\mathrm{s}, \cos\vartheta_\mathrm{s}]^\mathrm{T}$ expressed as a unit vector using angular coordinates, azimuth φ_s and zenith ϑ_s. Any panning function should achieve panning-invariant loudness and width and a directional mapping aligned with $\boldsymbol{\theta}_\mathrm{s}$.

Loudness and localization measures As RMS measures predict loudness well in practice [25],

$$E = \sum_{l=1}^{\mathrm{L}} g_l^2(\boldsymbol{\theta}_\mathrm{s}) \tag{2}$$

introduced by [17] will be used to inspect the loudness variation of a panning function. Frank's experiments proved the reliability of Gerzon's vector measure

$$\boldsymbol{r}_\mathrm{E} = \frac{\sum_{l=1}^{\mathrm{L}} g_l^2(\boldsymbol{\theta}_\mathrm{s})\,\boldsymbol{\theta}_l}{E}, \tag{3}$$

in terms of auditory localization and width [26, 27, 28]. It requires to know the unit vectors of the loudspeaker directions $\{\boldsymbol{\theta}_l\}$ in addition to the panning function.

We desire a unity loudness measure $E=1$, localization aligned with the panning direction $\boldsymbol{r}_\mathrm{E} \parallel \boldsymbol{\theta}_\mathrm{s}$, and of constant spread $\arccos\|\boldsymbol{r}_\mathrm{E}\| = \text{const.}$, if possible.

3 Virtual Ambisonic panning

In Ambisonics, there is an underlying continuous-direction ($\hat{\boldsymbol{\theta}}$) *virtual surround signal* obtained by a *virtual Ambisonic panning function* [6]

$$\hat{x}(t,\hat{\boldsymbol{\theta}}) = \hat{g}(\hat{\boldsymbol{\theta}},\boldsymbol{\theta}_\mathrm{s})\, s(t). \tag{4}$$

This *virtual Ambisonic panning function*

$$\hat{g}(\hat{\boldsymbol{\theta}},\boldsymbol{\theta}_\mathrm{s}) = \boldsymbol{y}_\mathrm{N}^\mathrm{T}(\hat{\boldsymbol{\theta}})\,\mathrm{diag}\{\boldsymbol{a}_\mathrm{N}\}\,\boldsymbol{y}_\mathrm{N}(\boldsymbol{\theta}_\mathrm{s}) \tag{5}$$

includes the encoder $\boldsymbol{y}_\mathrm{N}(\boldsymbol{\theta}_\mathrm{s}) = [Y_0^0(\boldsymbol{\theta}_\mathrm{s}),\ldots,Y_\mathrm{N}^\mathrm{N}(\boldsymbol{\theta}_\mathrm{s})]^\mathrm{T}$, a vector of N3D-normalized spherical harmonics up to the order N evaluated at the panning direction, and a *virtual decoder* $\boldsymbol{y}_\mathrm{N}^\mathrm{T}(\hat{\boldsymbol{\theta}})$ evaluating the spherical harmonics at a continuous direction $\hat{\boldsymbol{\theta}}$, and a sidelobe-suppressing max-$\boldsymbol{r}_\mathrm{E}$ weighting $\boldsymbol{a}_\mathrm{N} = [a_n]_{nm}$, cf. [1, 10], which consists of Legendre polynomials $P_n(\|\boldsymbol{r}_\mathrm{E}\|_\mathrm{max})$ that we define to be $\sqrt{E}$-normalized for simplicity

$$a_n = \frac{P_n(\cos\frac{137.9^\circ}{\mathrm{N}+1.51})}{\sqrt{\frac{\sum_{n=0}^{\mathrm{N}}(2n+1)\,[P_n(\cos\frac{137.9^\circ}{\mathrm{N}+1.51})]^2}{4\pi}}}. \tag{6}$$

This *virtual Ambisonic panning function* is ideal with optimally panning-invariant loudness measure, cf. [10],

$$\hat{E} = \int_{\mathbb{S}^2} g^2(\hat{\boldsymbol{\theta}},\boldsymbol{\theta}_\mathrm{s})\,\mathrm{d}\hat{\boldsymbol{\theta}} = 1, \tag{7}$$

and a localization measure of constant length and perfect alignment to $\boldsymbol{\theta}_\mathrm{s}$, indicating constant perceived width and $\boldsymbol{\theta}_\mathrm{s}$ as the perceived direction,

$$\hat{\boldsymbol{r}}_\mathrm{E} = \frac{\int_{\mathbb{S}^2} g^2(\hat{\boldsymbol{\theta}},\boldsymbol{\theta}_\mathrm{s})\,\hat{\boldsymbol{\theta}}\,\mathrm{d}\hat{\boldsymbol{\theta}}}{E} = \cos(\tfrac{137.9^\circ}{\mathrm{N}+1.51})\,\boldsymbol{\theta}_\mathrm{s}. \tag{8}$$

4 Ambisonic panning: integral over discretization kernel

For Ambisonic panning, the *virtual Ambisonic panning function* needs to produce discrete surround signals. As implied in [7, 8, 9, 10, 11, 16], this can be done by an integral of the *virtual Ambisonic panning function* over a *discretization kernel* $\hat{K}_l(\hat{\boldsymbol{\theta}})$ for each loudspeaker l

$$g_l(\boldsymbol{\theta}_\mathrm{s}) = \int_{\mathbb{S}^2} \hat{K}_l(\hat{\boldsymbol{\theta}})\,\hat{g}(\hat{\boldsymbol{\theta}},\boldsymbol{\theta}_\mathrm{s})\,\mathrm{d}\hat{\boldsymbol{\theta}}. \tag{9}$$

The *discretization kernel* $\hat{K}_l(\hat{\boldsymbol{\theta}})$ acts as a beam shape collecting the l^th loudspeaker's signal from the *virtual surround signal*.

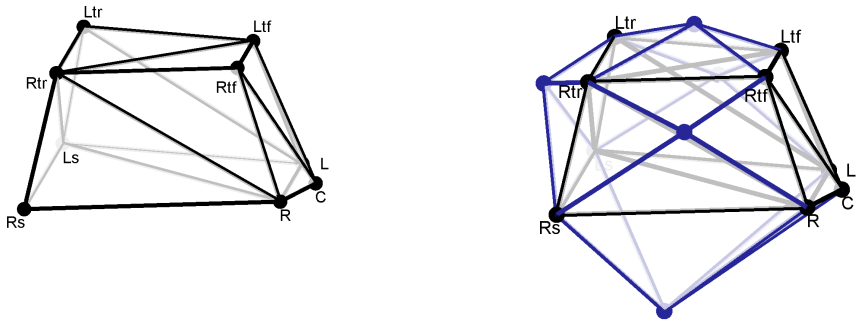

Fig. 2: Convex hull of the 4+5+0 loudspeaker layout without and with imaginary loudspeakers.

Numerical integration With an N^{th}-order *virtual Ambisonic panning function* and assuming the kernel $\hat{K}_l(\hat{\boldsymbol{\theta}})$ to be of the Q^{th} order, a t-design with $t \geq \mathrm{Q}+\mathrm{N}$ provides an exact numerical integration rule to evaluate Ambisonic panning in Eq. (9). With a t-design consisting of J discrete directions $\{\hat{\boldsymbol{\theta}}_j\}$ we obtain

$$g_l(\boldsymbol{\theta}_\mathrm{s}) = \sum_{j=1}^{\mathrm{J}} \hat{K}_l(\hat{\boldsymbol{\theta}}_j)\, \hat{g}(\hat{\boldsymbol{\theta}}, \boldsymbol{\theta}_\mathrm{s})\, \tfrac{4\pi}{\mathrm{J}}. \qquad (10)$$

If the discretization kernel is smooth enough, a $\mathrm{J} = 5200$ nodes Chebyshev-type quadrature from Gräf [29] can achieve reasonably accurate results in practice.

Examples for $\hat{K}(\hat{\boldsymbol{\theta}})$ *Which designs for $\hat{K}_l(\hat{\boldsymbol{\theta}})$ yield Ambisonic panning with reasonable E and $\boldsymbol{r}_\mathrm{E}$ measures?* For Ambisonic panning by sampling, the discretization kernel simply consists of a Dirac delta distribution $\hat{K}_l(\hat{\boldsymbol{\theta}}) = \delta(\hat{\boldsymbol{\theta}} - \boldsymbol{\theta}_l)$ that samples the *virtual Ambisonic panning function* $g_l(\boldsymbol{\theta}_\mathrm{s}) = \hat{g}(\boldsymbol{\theta}_l, \boldsymbol{\theta}_\mathrm{s})$ at the l^{th} loudspeaker direction $\boldsymbol{\theta}_l$. This is not always a good choice, cf. [10, 11], as it would require an optimal loudspeaker layout. Only so-called t-designs of the parameter $t \geq 2\mathrm{N}+1$, cf. [29], are layouts suitable for sampling with perfect E and $\boldsymbol{r}_\mathrm{E}$ measures, cf. [10].

For more general layouts, other discretization kernels are preferable. For instance, in [7, 8, 9, 10, 11], the discretization kernel is the vector-base amplitude panning function $\hat{K}_l(\hat{\boldsymbol{\theta}}) = \hat{g}_{\mathrm{VBAP},l}(\hat{\boldsymbol{\theta}})$ with extensions, and in [16], it is an optimized multiple-direction amplitude panning [30] function $\hat{K}_l(\hat{\boldsymbol{\theta}}) = \hat{g}_{\mathrm{MDAP},l}(\hat{\boldsymbol{\theta}})$.

4.1 AllRAP: VBAP discretization kernel

All-Round Ambisonic Panning (AllRAP) employs VBAP gains as discretization kernel. VBAP requires to identify which loudspeaker triplets form a triangle of neighboring loudspeakers. Such triplets are best defined by the convex hull $H_{k,j}$, cf. Fig. 2, that holds loudspeaker indices depending on the triangle k and triangle vertices $j = 0, 1, 2$. The VBAP gains result from a loop searching for the first triplet with all-positive weights:

$$k = 0, \qquad (11)$$

while k<size(H_{kl},k) {

$\forall l: \quad \hat{g}_l = 0, \qquad \boldsymbol{L}_k = [\boldsymbol{\theta}_{H_{k,1}}, \boldsymbol{\theta}_{H_{k,2}}, \boldsymbol{\theta}_{H_{k,3}}],$

$[\hat{g}_l]_{l=H_{k,1\ldots3}} = \boldsymbol{L}_k^{-1}\, \hat{\boldsymbol{\theta}}, \quad$ stop if $\hat{g}_{H_{k,1}}, \hat{g}_{H_{k,2}}, \hat{g}_{H_{k,3}} \geq 0,$

k++ }

normalize $\hat{g}_{\mathrm{VBAP},l}(\hat{\boldsymbol{\theta}}) = \hat{g}_l \big/ \sqrt{\sum_{l=1}^{\mathrm{L}} \hat{g}_l^2}$.

In AllRAP, the higher the Ambisonic order is chosen, the more the result will resemble VBAP. AllRAP will not be all perfect but it can be adjusted easily to the geometrical particularities of the loudspeaker layout.

AllRAP on ITU BS.2051 4+5+0: VBAP and imaginary loudspeaker downmix The triangulation of the 4+5+0 loudspeaker layout is shown in Fig. 2 (left), and it is typically modified by the insertion of 5 imaginary loudspeakers into the convex hull (right).

An imaginary loudspeaker is inserted at nadir $[x,y,z] = 0.72\,[0,0,-1]$ to preserve signals slightly below the horizon, and its signal will not be downmixed but discarded. Moreover, our current algorithm inserts 4 more imaginary loudspeakers in the mean direction of each of the quadrilaterals at the sides $0.93\,[0.22, \pm 0.83, 0.51]$, in the back $0.88\,[-0.77, 0, 0.64]$ and on top $0.94\,[0.18, 0, 0.98]$. The slightly recessed radius is only for the convex hull algorithm to keep the quadrilateral areas separate, and it will be removed for VBAP. Each of these imaginary loudspeakers' signals is mixed down to its 4 neighboring loudspeakers with the factor $\frac{1}{\sqrt{4}}$. For directions falling into the downmixed quadrilaterals, the resulting panning gains of the real loudspeakers can moreover be re-normalized to perfectly achieve $\sum_{l=0}^{\mathrm{L}} \hat{g}_{\mathrm{VBAP},l}^2 = 1$.

Despite the successful effort of imaginary loudspeaker insertion and downmix, panning to the back yields an E measure (loudness) indicating $+2.75$ dB when compared to panning to the front, see Fig. 3 (top).

Although both, the *virtual Ambisonic panning function* and the VBAP *discretization kernel* yield ideal loudness $\hat{E} = \int \hat{g}(\hat{\boldsymbol{\theta}}, \boldsymbol{\theta}_\mathrm{s})^2 \,\mathrm{d}\hat{\boldsymbol{\theta}} = 1$ and $E = \sum_l \hat{g}^2_{\mathrm{VBAP},l}(\hat{\boldsymbol{\theta}}) = 1$, their linear combination is not ideal. In particular, triangles at back, sides, and top are substantially larger than those in front. By constructive superposition they cause larger results than a stochastic superposition.

4.2 AllRAP2^2 and AllRAP2

Without changing the ideal value $\hat{E} = 1$, the integrand in Eq. (7) is expanded by unity, to which squared VBAP gains sum up $\overbrace{\sum_{l=1}^{\mathrm{L}} \hat{g}^2_{\mathrm{VBAP},l}(\hat{\boldsymbol{\theta}})}^{} = 1$ in the panning range,

$$\hat{E} = \int_{\mathbb{S}^2} \overbrace{\sum_{l=1}^{\mathrm{L}} \hat{g}^2_{\mathrm{VBAP},l}(\hat{\boldsymbol{\theta}})}^{} \; \hat{g}^2(\hat{\boldsymbol{\theta}}, \boldsymbol{\theta}_\mathrm{s}) \,\mathrm{d}\hat{\boldsymbol{\theta}} = 1.$$

Re-arranging sum and integral yields

$$\hat{E} = \sum_{l=0}^{\mathrm{L}} \underbrace{\left[\int_{\mathbb{S}^2} \hat{g}^2_{\mathrm{VBAP},l}(\hat{\boldsymbol{\theta}}) \, \hat{g}^2(\hat{\boldsymbol{\theta}}, \boldsymbol{\theta}_\mathrm{s}) \,\mathrm{d}\hat{\boldsymbol{\theta}} \right]}_{g^2_{\mathrm{AllRAP2}^2,l}} = 1,$$

and defines the squared AllRAP2^2 panning function

$$\hat{g}^2_{\mathrm{AllRAP2}^2,l}(\boldsymbol{\theta}_\mathrm{s}) = \int_{\mathbb{S}^2} \hat{g}^2_{\mathrm{VBAP},l}(\hat{\boldsymbol{\theta}}) \, \hat{g}^2(\hat{\boldsymbol{\theta}}, \boldsymbol{\theta}_\mathrm{s}) \,\mathrm{d}\hat{\boldsymbol{\theta}} \quad (12)$$

of panning-invariant loudness, wherever it was panning-invariant with VBAP. Obviously, Eq. (12) runs an integral of the squared virtual Ambisonic panning function over a squared VBAP discretization kernel, which can be evaluated numerically similarly as in Eq. (10), however it is not a linear Ambisonic panning function yet.

AllRAP2 To generate the linear Ambisonic panning function AllRAP2 from AllRAP2^2 Eq. (12), we use another integral Eq. (9) or (10) with the positive square-root $\hat{K}_l(\hat{\boldsymbol{\theta}}) = \overset{+}{(-)}\sqrt{\hat{g}^2_{\mathrm{AllRAP2}^2,l}(\hat{\boldsymbol{\theta}})}$ as linear kernel.

5 Ambisonic decoding, AllRAD and AllRAD2

All the sections above dealt with Ambisonic panning functions using the integral in Eq. (9) or numerical integral in Eq. (10), to keep things as compact as possible. To finally establish the important connection to a fully equivalent Ambisonic decoder, whose improved computation is the foremost intention of this contribution, we insert the virtual Ambisonic panning function Eq. (5) into the integral of the Ambisonic panning function of Eq. (9). We gather the part of the result that defines the l^{th} row of the equivalent decoder $\boldsymbol{D} = [\boldsymbol{d}_l]^{\mathrm{T}}_l$,

$$g_l(\boldsymbol{\theta}_\mathrm{s}) = \boldsymbol{d}_l^{\mathrm{T}} \, \boldsymbol{y}_\mathrm{N}(\boldsymbol{\theta}_\mathrm{s}),$$
$$\boldsymbol{d}_l^{\mathrm{T}} = \int_{\mathbb{S}^2} \hat{K}_l(\hat{\boldsymbol{\theta}}) \, \boldsymbol{y}_\mathrm{N}^{\mathrm{T}}(\hat{\boldsymbol{\theta}}) \,\mathrm{d}\hat{\boldsymbol{\theta}} \; \mathrm{diag}\{\boldsymbol{a}_\mathrm{N}\}, \quad (13)$$

which is the max-$\boldsymbol{r}_\mathrm{E}$-weighted spherical harmonic transformation of the discretization kernel $\hat{K}_l(\hat{\boldsymbol{\theta}})$.

AllRAD AllRAD constructs an Ambisonic decoder by employing VBAP with imaginary loudspeakers as the discretization kernel $\hat{K}_l(\hat{\boldsymbol{\theta}}) = \hat{g}_{\mathrm{VBAP},l}(\hat{\boldsymbol{\theta}})$ to calculate a decoder by Eq. (13). By imaginary loudspeaker insertion and downmix in its VBAP part, it permits large freedom to adapt to special loudspeaker layouts.

AllRAD2 AllRAD2 constructs an optimally loudness preserving decoder, also by using VBAP with imaginary loudspeakers as discretization kernel, but it first does so in a domain of squares to ideally preserve loudness. This yields a squared panning function AllRAP2^2 Eq. (12) solved by numerical integration. The positive square root of its result is used as discretization kernel $\hat{K}_l(\hat{\boldsymbol{\theta}}) = \overset{+}{(-)}\sqrt{\hat{g}^2_{\mathrm{AllRAP2}^2,l}(\hat{\boldsymbol{\theta}})}$ for a second integral by Eq. (13), whose numerical integration yields AllRAD2. Numerical integration is best done just as in Eq. (10).

6 Discussion

Figs. 3,4 (top) compare E measures obtained for AllRAD with imaginary loudspeakers and the two-stage approach of AllRAD2. For both figures, the number top left measures the loudness span $\max\{E\} - \min\{E\}$ for panning on the upper hemisphere, which obviously reduced from 2.75 dB (AllRAD) to 0.22 dB (AllRAD2).

Figs. 3,4 (middle) compare the width measure $\arccos \|\boldsymbol{r}_\mathrm{E}\|$ of panning by AllRAD and AllRAD2. The number top left indicates minimum, median, and maximum of the spread $\arccos \|\boldsymbol{r}_\mathrm{E}\|$ in degrees in the important frontal panning range for azimuth angles $\varphi \in [-45°; +45°]$ and zenith angles $\vartheta \in [30°; 90°]$. Obviously AllRAD2 causes a minimum/median/maximum spread in this range that is approximately 4° larger and $23°/30°/39°$ instead of $18°/26°/36°$; which is a relatively small widening, only.

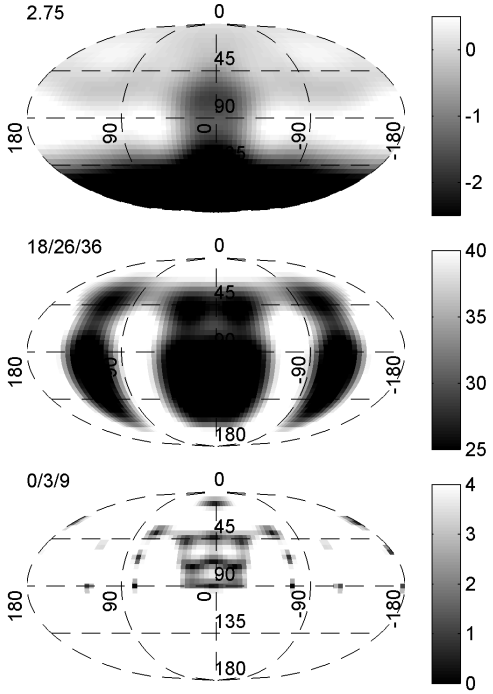

Fig. 3: Analysis: 5th-order AllRAD over the panning direction $\boldsymbol{\theta}_\mathrm{s}$ in terms of E in dB (top), angular spread $\arccos\|\boldsymbol{r}_\mathrm{E}\|$ in degrees (middle) and angular error $\arccos\frac{\boldsymbol{\theta}_\mathrm{s}^\mathrm{T}\boldsymbol{r}_\mathrm{E}}{\|\boldsymbol{r}_\mathrm{E}\|}$ in degrees (bottom).

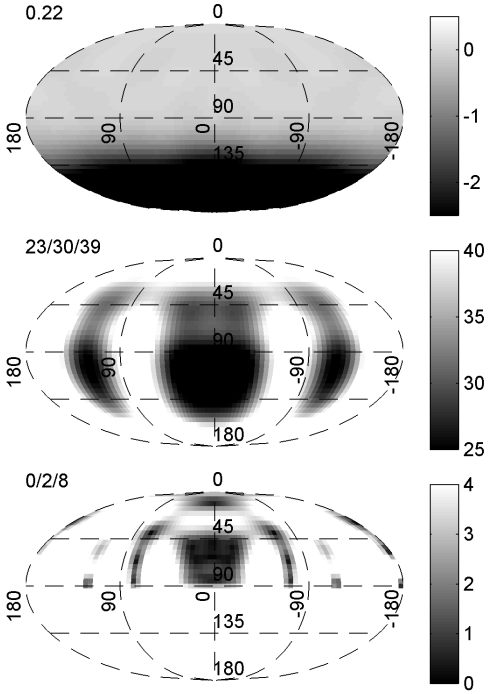

Fig. 4: Analysis: 5th-order AllRAD2 over the panning direction $\boldsymbol{\theta}_\mathrm{s}$ in terms of E in dB (top), angular spread $\arccos\|\boldsymbol{r}_\mathrm{E}\|$ in degrees (middle) and angular error $\arccos\frac{\boldsymbol{\theta}_\mathrm{s}^\mathrm{T}\boldsymbol{r}_\mathrm{E}}{\|\boldsymbol{r}_\mathrm{E}\|}$ in degrees (bottom).

Figs. 3,4 (bottom) compare the directional mapping error $\arccos\frac{\boldsymbol{\theta}_\mathrm{s}^\mathrm{T}\boldsymbol{r}_\mathrm{E}}{\|\boldsymbol{r}_\mathrm{E}\|}$ of panning by AllRAD and AllRAD. The number top left indicates minimum, median, and maximum of this error in degrees, again for the important frontal panning range $\varphi \in [-45°;+45°]$ and $\vartheta \in [30°;90°]$. Interestingly AllRAD2 causes a minimum/median/maximum spread in this range that is approximately 1° smaller. Despite this is surprising, it is a negligible improvement.

7 Summary

We presented AllRAD2 decoding achieving a panning-invariant loudness on standard 3D loudspeaker setups of small loudspeaker number and typically largely varying loudspeaker spacings. Despite panning and decoding with All-Round Ambisonic Decoding (AllRAD) is appreciated for its flexibility, it yields a loudness difference that is worth discussing: 2.75 dB between front and back on the 4+5+0 ITU BS.2051 layout for 5th-order max-$\boldsymbol{r}_\mathrm{E}$ Ambisonics. The AllRAD2 approach is able to reduce the loudness difference to 0.22 dB.

The new method AllRAD2 only weakly degrades the width measure by a slight increase from 26° to 30° for frontal panning, which level meters show in terms of a weaker attenuation of back and side channels.

Informal listening to a 4+5+0 loudspeaker subset at IEM's production studio confirms the improved panning invariance of loudness of AllRAD2 compared to AllRAD, while no changes of localization and width were perceived at typical listening positions. For layouts with more and regularly spaced loudspeakers, where loudness already varies by less than 1 dB, we advise to keep AllRAD, its narrower source width, and its high channel separation.

Formally, we expressed Ambisonic decoding as integral transform over a discretization kernel $\hat{K}_l(\hat{\boldsymbol{\theta}})$ that directionally gathers loudspeaker signals from the direction-continuous virtual Ambisonic surround signal. This might inspire new decoding approaches and implies a resulting beampattern for every loudspeaker as in [7, 8].

Acknowledgment

We thank Frank Schultz for critical proof reading.

References

[1] Daniel, J., Rault, J.-B., and Polack, J.-D., "Ambisonics Encoding of Other Audio Formats for Multiple Listening Conditions," in *prepr. 4795, 105th AES Conv.*, 1998.

[2] Daniel, J., *Repréesentation de champs acoustiques, application à la transmission et à la reproduction de scénes sonores complexes dans un contexte multimédia*, Ph.D. thesis, Université Paris 6, 2001.

[3] Poletti, M. A., "A Unified Theory of Horizontal Holographic Sound Systems," *J. Audio Eng. Soc.*, 48(12), pp. 1155–1182, 2000.

[4] Poletti, M. A., "Three-Dimensional Surround Sound Systems Based on Spherical Harmonics," *J. Audio Eng. Soc*, 53(11), pp. 1004–1025, 2005.

[5] Poletti, M. A., "Robust two-dimensional surround sound reproduction for nonuniform loudspeaker layouts," *J. Audio Eng. Soc.*, 55(7/8), pp. 598–610, 2007.

[6] Zotter, F., Pomberger, H., and Noisternig, M., "Energy-Preserving Ambisonic Decoding," *Acta Acustica united with Acustica*, 98(1), pp. 37–47, 2012.

[7] Batke, J.-M. and Keiler, F., "Investigation of Robust Panning Functions for 3-D Loudspeaker Setups," in *prepr. 7979, 128th AES Conv.*, 2010.

[8] Batke, J.-M. and Keiler, F., "Using VBAP-derived panning functions for 3D ambisonics decoding," in *Proc. 2nd Int. Symp. Ambisonics and Spherical Acoustics*, Paris, 2010.

[9] Zotter, F., Frank, M., and Sontacchi, A., "The virtual t-design Ambisonics-rig using VBAP," in *Proc. 1st EAA-EuroRegio*, Ljubljana, 2010.

[10] Zotter, F. and Frank, M., "All-Round Ambisonic panning and decoding," *J. Audio Eng. Soc.*, 60(10), pp. 807–820, 2012.

[11] Zotter, F., Frank, M., and Pomberger, H., "Comparison of Energy-Preserving and All-Round Ambisonic Decoders," in *Fortschritte der Akustik - AIA/DAGA, Meran*, 2013.

[12] Moore, D. and Wakefield, J., "A design tool to produce optimized Ambisonic decoders," in *4th Int. AES Conf.*, Tokyo, 2010.

[13] Scaini, D. and Arteaga, D., "An Evaluation of the IDHOA Ambisonics Decoder in Irregular Planar Layouts," in *pepr. 9249m 138th AES Conv.*, Kraków, 2015.

[14] Heller, A. K., Benjamin, E. M., and Lee, R., "Design of Ambisonic Decoders for Irregular Arrays of Loudspeakers by Non-Linear Optimization," in *prepr. 8243, 129th AES Conv.*, San Francisco, 2010.

[15] Heller, A. K. and Benjamin, E. M., "The Ambisonic decoder toolbox," in *Linux Audio Conference*, Karlsruhe, 2014.

[16] Epain, N., Jin, C. T., and Zotter, F., "Ambisonic Decoding With Constant Angular Spread," *Acta Acustica united with Acustica*, 100(5), pp. 928–936, 2014.

[17] Gerzon, M. A., "General metatheory of auditory localisation," in *prepr. 3306, 92nd AES Conv.*, Vienna, 1992.

[18] Craven, P., "Continuous Surround Panning for 5-speaker Reproduction," in *24th AES Int. Conf.*, Banff, 2003.

[19] Wiggins, B., Berry, S., and Lowndes, V., "The design and optimisation of surround sound decoders using heuristic methods," in *Proc. UKSim 2003, Conference of the UK Simulation Society*, pp. 106—-114, 2003.

[20] ITU, "Recommendation BS.2051 - Advanced sound system for programme production," 2017.

[21] Romanov, M., Frank, M., Zotter, F., and Nixon, T., "Manipulations improving amplitude panning on small standard loudspeaker arrangements for surround with height," in *29th Tonmeistertagung*, Köln, 2016.

[22] Romanov, M., Zotter, F., Frank, M., and Pike, C., "Comparison of spatial audio rendering methods for ITU-R BS. 2051 standard loudspeaker layouts," in *Proc. 4th Int. Conf. Spatial Audio (ICSA)*, Graz, 2017.

[23] Frank, M. and Sontacchi, A., "Case Study on Ambisonics for Multi-Venue and Multi-Target Concerts and Broadcasts," *J. Audio Eng. Soc.*, 65(9), pp. 749–756, 2017.

[24] Pulkki, V., "Virtual Sound Source Positioning Using Vector Base Amplitude Panning," *Journal of Audio Engineering Society*, 45(6), pp. 456–466, 1997.

[25] Soulodre, G., "Evaluation of Objective Measures of Loudness," in *prepr. 6161, 116th AES Conv.*, Berlin, 2004.

[26] Frank, M., *Phantom Sources using Multiple Loudspeakers in the Horizontal Plane*, Ph.D. thesis, University of Music and Performing Arts, Graz, Inst. Electronic Music and Acoustics, 2013.

[27] Frank, M., "Source width of frontal phantom sources: Perception, measurement, and modeling," *Archives of Acoustics*, 38(3), pp. 311–319, 2013.

[28] Frank, M., "Localization using different amplitude-panning methods in the frontal horizontal plane," in *Proc. EAA Symposium on Auralization and Ambisonics*, Berlin, 2014.

[29] Gräf, M. and Potts, D., "On the computation of spherical designs by a new optimization approach based on fast spherical Fourier transforms," *Numer. Math.*, 119, pp. 699–724, 2011.

[30] Pulkki, V., "Uniform spreading of amplitude panned virtual sources," in *Applications of Signal Processing to Audio and Acoustics, 1999 IEEE Workshop on*, pp. 187–190, 1999.